Sensitivity of Circulation in the Skagit River Estuary to Sea Level Rise and Future Flows

Authors: Khangaonkar, Tarang, Long, Wen, Sackmann, Brandon, Mohamedali, Teizeen, and Hamlet, Alan F.

Source: Northwest Science, 90(1) : 94-118

Published By: Northwest Scientific Association

URL: https://doi.org/10.3955/046.090.0108

Tarang Khangaonkar[1], Pacific Northwest National Laboratory, Marine Sciences Division, 1100 Dexter Avenue North, Suite 400, Seattle, Washington 98109

Wen Long, Pacific Northwest National Laboratory, Marine Sciences Division, 1100 Dexter Avenue North, Suite 400, Seattle, Washington 98109

Brandon Sackmann, Integral Counseling Inc., 1205 West Bay Drive, Olympia, Washington 98502

Teizeen Mohamedali, Washington State Department of Ecology, P.O. Box 47600, Olympia, Washington 98504

and

Alan F. Hamlet, University of Notre Dame, Department of Civil and Environmental Engineering and Earth Sciences, 156 Fitzpatrick Hall, University of Notre Dame, Notre Dame, Indiana 46556

Sensitivity of Circulation in the Skagit River Estuary to Sea Level Rise and Future Flows

Abstract

Future climate simulations based on the Intergovernmental Panel on Climate Change emissions scenario (A1B) have shown that the Skagit River flow will be affected, which may lead to modification of the estuarine hydrodynamics. There is considerable uncertainty, however, about the extent and magnitude of resulting change, given accompanying sea level rise and site-specific complexities with multiple interconnected basins. To help quantify the future hydrodynamic response, we developed a three-dimensional model of the Skagit River estuary using the Finite Volume Community Ocean Model (FVCOM). The model was set up with localized high-resolution grids in Skagit and Padilla Bay sub-basins within the intermediate-scale FVCOM based model of the Salish Sea (greater Puget Sound and Georgia Basin). Future changes to salinity and annual transport through the basin were examined. The results confirmed the existence of a residual estuarine flow that enters Skagit Bay from Saratoga Passage to the south and exits through Deception Pass. Freshwater from the Skagit River is transported out in the surface layers primarily through Deception Pass and Saratoga Passage, and only a small fraction (~ 4%) is transported to Padilla Bay. The moderate future perturbations of A1B emissions, corresponding river flow, and sea level rise of 0.48 m examined here result only in small incremental changes to salinity structure and inter-basin freshwater distribution and transport. An increase in salinity of ~1 psu in the near-shore environment and a salinity intrusion of approximately 3 km further upstream is predicted in Skagit River, well downstream of drinking water intakes.

Keywords: sea level rise, future hydrology, estuarine circulation, Skagit River, salinity intrusion

Introduction

Coastal ecosystems in the Pacific Northwest (PNW) are composed of numerous tide flats, marshes, and eelgrass beds that support thousands of species of fish and wildlife, which in turn are vital to the regional economy, culture, and quality of life in the PNW. These habitats are present in the large and complex estuarine reaches within the Salish Sea, which includes Puget Sound, the Strait of Juan de Fuca, the Georgia Strait, and adjacent Canadian waters. Potential changes to coastal physical processes such as inundation, circulation, hydrodynamic transport, and bio-geochemical cycles as a result of climate change and sea level rise are of utmost importance here; therefore, adaptive management actions must be considered to ensure long-term coastal protection and sustainable use of the near-shore resources (National Wildlife Federation 2007). Over oceanic scales, the effects of climate change, including sea level rise, increased stratification, and alteration to precipitation and freshwater inputs are expected to affect patterns of circulation, thus leading to numerous ecosystem impacts (Doney et al. 2011, National Research Council 2011). On a smaller riverine or estuarine scale, however, responses may vary based on site-specific conditions. In the

[1]Author to whom correspondence should be addressed.
Email: tarang.khangaonkar@pnnl.gov

absence of information on local hydrodynamic and environmental characteristics, community-wide uncertainty about the magnitude of potential future impacts often hinders efforts to plan and implement adaptive management measures.

This is the case in the Skagit River estuary, a sub-basin within Puget Sound, where many near-shore and estuarine habitat restoration and protection projects are underway with the goal of recovering wild salmon populations from historically low levels. Fisheries biologists using local Chinook salmon data have established that returns in the Skagit River can be predicted with high precision through analysis of habitat and residence data. Numerous biological monitoring studies in the Skagit River estuary have helped generate information on the taxonomic composition of fish assemblages, juvenile salmon density, size, and origin for differing physical habitat and salinity (e.g., Beamer et al. 2005a, 2005b, 2007; Rice 2007). Availability of freshwater supply and near-shore environmental conditions are also known to significantly influence the survival of Skagit River Chinook salmon (Greene et al. 2005). However, historical measurements of water movement through the estuary are limited. Detailed understanding of the circulation and hydrodynamic conditions in the Skagit River estuary, and its interaction with Padilla Bay to the north and Saratoga Passage to the south, are only beginning to emerge through short-duration synoptic measurements of currents, tides, salinities, and temperatures (Yang and Khangaonkar 2006, Grossman et al. 2007). A thorough characterization of baseline estuarine and coastal hydrodynamics including long-term seasonal variations is essential to support the design and development of habitat restoration and land use plans for successful recovery of fish populations. The future success of proposed restoration actions may then be assessed based on sensitivity of circulation and transport in the Skagit River estuary to sea level rise and future climate loads.

Circulation and transport are naturally complex in the Skagit River estuary because of its unique oceanographic setting. The estuary is located at the north end of the Whidbey Basin, which is the body of water enclosed by Whidbey Island and the east coast of Puget Sound (Figure 1). The east coast of Puget Sound also hosts two other major estuaries, the Stillaguamish River and the Snohomish River estuaries. Pacific tides enter the Salish Sea through the Strait of Juan de Fuca and propagate to Skagit Bay via three pathways: 1) from Padilla Bay at the north boundary through Swinomish Channel, 2) through Deception Pass, and 3) south into Puget Sound over Admiralty Inlet, around Whidbey Island and north into Skagit Bay through Saratoga Passage. The resulting tides in Skagit Bay exhibit mixed, semi-diurnal dominant characteristics, and show large inequalities in tidal range and a strong spring-neap tidal cycle. The three tidal pathways introduce phase effects on the tidal forcing and movement throughout the estuary.

The Skagit River is the largest river to flow into Puget Sound with a drainage area of about 8,000 km^2. Depending on the season, the Skagit River is responsible for approximately 34 to 50% of the total riverine freshwater flow into Puget Sound (Hood 2006, Babson et al. 2006, Cannon 1983). The river flow peaks both in winter (because of runoff), and again in late spring or early summer (because of snow melt), and is often at a minimum in September. The mean flow of the Skagit River at Mt. Vernon, Washington, is 468 m^3/s, with recorded maximum and minimum flows of 5100 m^3/s and 78 m^3/s, respectively (Wiggins et al. 1997). The Skagit River splits into the North Fork and the South Fork distributaries before it enters Skagit Bay. The North Fork channel runs westerly as a dike-bounded conduit through the marshlands, while the South Fork enters Skagit Bay through multiple small tidal distributary channels. The central region of the Skagit River delta in between the North and South Forks has been diked through historical agricultural developments and is known as Fir Island. Because of soil compaction that affects drainage of precipitation and irrigation water, the enclosed agricultural land has undergone subsidence of up to 1.2 m locally over the last century. The dikes also have impeded fish passage through the area and greatly reduced nursery habitat for many fish and invertebrates (Beamer et al. 2005a). A large tidal flat exists seaward of the Fir Island dike and most of the northeastern region of Skagit Bay is above the

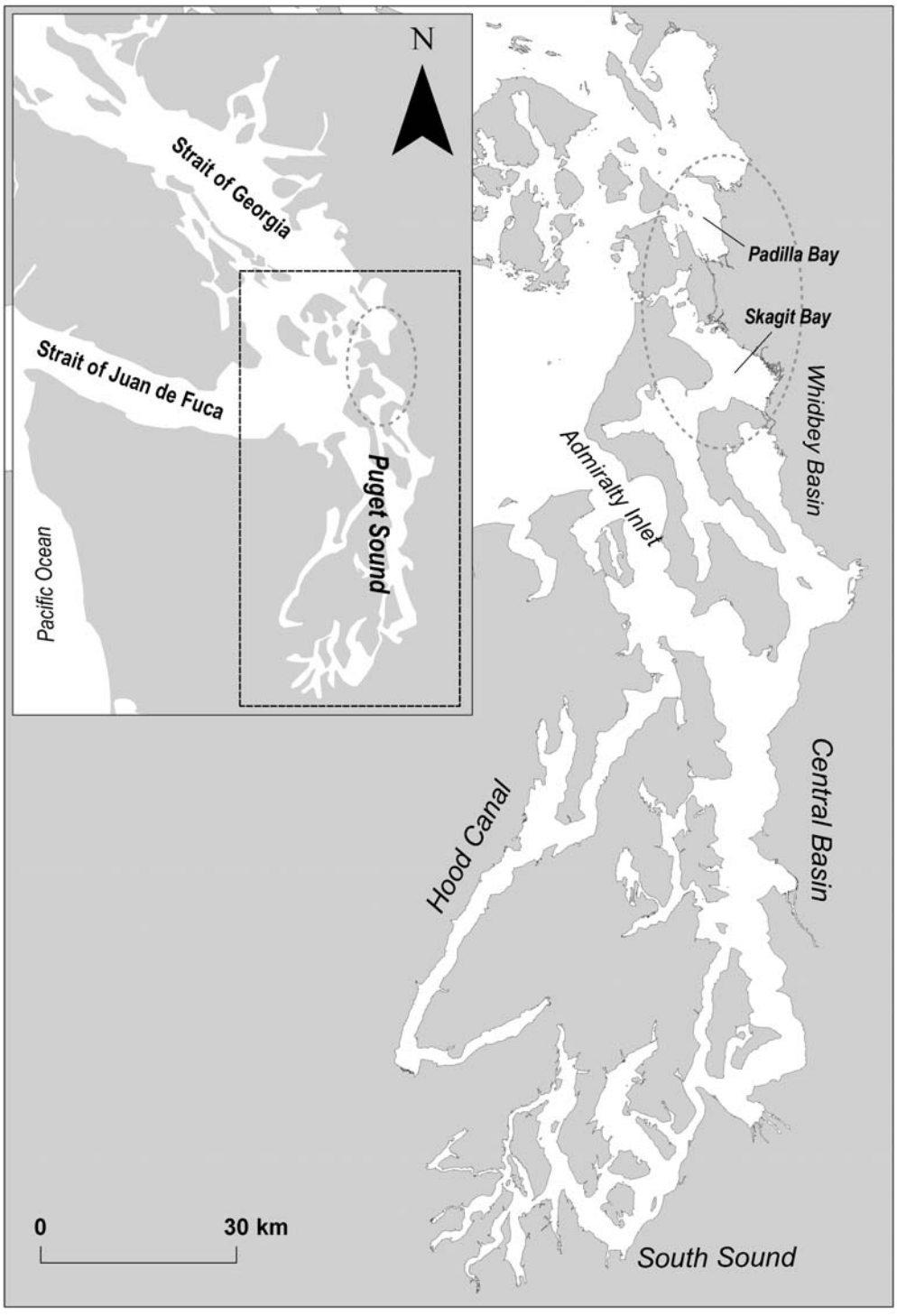

Figure 1. Oceanographic regions of Puget Sound and Georgia Basin (collectively known as the Salish Sea) including the study area of Skagit Bay and Padilla Bay system within the Whidbey Basin.

mean lower low water line. A relatively deep and narrow channel (25 to 30 m) exists between the east coast of Whidbey Island and the tidal flats of Skagit Bay.

A three-dimensional (3-D) hydrodynamic model of the Skagit River estuary including Skagit Bay, the North Fork, the connection to Padilla Bay through Swinomish Channel, and the braided network associated with the South Fork was developed previously (Yang and Khangaonkar 2009). The model was developed using the Finite Volume Community Ocean Model (FVCOM) code (Chen et al. 2003), and includes a detailed representation of the tide flat bathymetry, river-training dikes and jetty, Swinomish navigation channel, and Skagit Bay. Simulation results from the model showed that tidal circulation and river plume dynamics in these shallow-water estuarine systems are affected strongly by the large intertidal zones. Strong asymmetries in tidal currents and stratification often occur in the intertidal zones and subtidal channels. Model calibration and validation then were conducted using the available short-duration current meter records from June 2005 and May 2006. Simulation results were consistent with the general understanding that the net transport of Skagit River water out of the basin is to the north through Deception Pass and the Swinomish Channel. However, subsequent independent modeling efforts of the Salish Sea-wide domain (Puget Sound and Georgia Basin) including Whidbey Basin and Skagit Bay indicated that net freshwater outflow in the surface layers from Skagit Bay was to the north during the winter and high-river-flow months but was to the south through Saratoga Passage through most of the remaining months of the year (Khangaonkar et al. 2011, Sutherland et al. 2011). Further examination indicated the possibility that previous Skagit Bay model results could have been affected by the short duration of simulation and inaccuracies with tidal phase at the model boundaries. To account for the possibility that the net transport direction may be influenced by seasonal variability in Skagit River inflow and wind forcing, a longer duration simulation was deemed necessary.

In this paper, we present an improved 3-D hydrodynamic analysis of circulation and transport in the Skagit River estuary including the interaction between the interconnected basins of Skagit Bay, Padilla Bay, and Saratoga Passage. This analysis includes a new synoptic data set of currents, tides, and salinities from year 2008 from the Skagit and Padilla Bays regions. The analysis was conducted using an existing model of the Salish Sea, improved with a high-resolution grid implemented for the Padilla Bay, Skagit Bay, and Saratoga Passage region. The baseline characteristics of tides, currents, and salinity gradients based on 2008 simulations were compared with results using future projections of sea level rise and hydrologic conditions as part of the sensitivity analysis. The effect of future conditions on upstream salinity intrusion and net transport through the system is presented below.

Methods

Model Setup

Embedded Fine-Scale Simulation of Skagit and Padilla Bay Sub-Basins—A hydrodynamic model of the interconnected Skagit and Padilla Bay sub-basins capable of resolving the fine-scale shoreline features, embedded within the existing larger intermediate-scale model of the Salish Sea, was developed for this analysis. The Salish Sea Model (SSM) uses the FVCOM framework (Chen et al. 2003) and has been discussed in detail previously (Khangaonkar et al. 2011, Khangaonkar et al. 2012). It uses an intermediate-scale grid constructed using triangular cells with higher resolution of 250 m in narrower inner basins, and then growing coarser in scale in the Strait of Juan de Fuca with up to 3-km resolution near the open boundary as shown in Figure 2. The primary ocean-side open boundary is located just west of the Strait of Juan de Fuca, while the second open boundary is near the northern end of the Georgia Strait (Canadian waters) near the entrance to Johnstone Straits. The model is forced by tides specified along the open boundaries using harmonic tide predictions (Flater 1996), freshwater inflows, wind, and heat flux at the water surface.

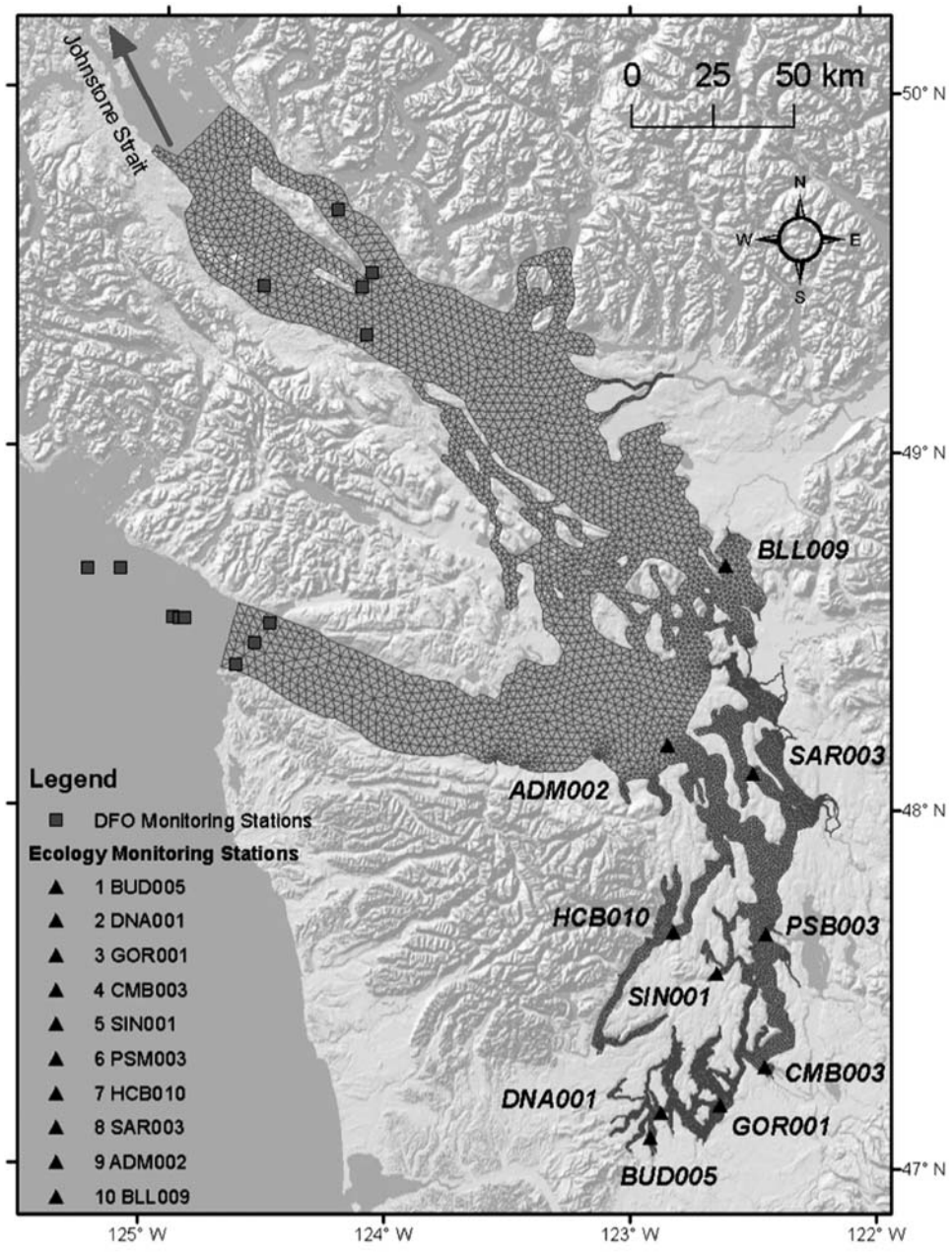

Figure 2. Intermediate-scale Salish Sea Model (SSM) grid.

The baseline year selected for this analysis was 2008 during which a short 2-week duration effort was expended to collect a synoptic oceanographic data set with stations deployed simultaneously in the Skagit as well as Padilla Bay regions. The meteorological parameters for year 2008 were obtained from the Weather Forecasting Research (WRF) model reanalysis data generated by the University of Washington. Temperature and salinity profiles along the open boundaries were specified based on monthly observations conducted by the department of Fisheries and Oceans, Canada,

during 2008. The SSM includes 19 gaged major rivers, 45 nonpoint source loads as estimated watershed stream flows, and 95 wastewater treatment plant discharges. The nonpoint source/watershed stream flows were estimated through a combination of measured stream-flow data and hydrologic modeling analysis conducted by Washington State Department of Ecology (Ecology) for the year 2008 (Mohamedali et al. 2011).

The embedded high-resolution grid model of the Skagit and Padilla Bay domain used in this study was based on a prior standalone model of Skagit Bay (Yang and Khangaonkar 2009) that was subsequently extended into Padilla Bay to the north and to Saratoga Passage to the south. It includes details such as river-training jetties, dikes, small islands, and connection to Padilla Bay through the Swinomish Channel using elements as small as 10 m in element length at selected locations. FVCOM has been applied successfully to numerous projects in the Puget Sound region using this grid scale in connection with nearshore restoration actions for improving the water quality and ecological health (Yang et al. 2010a, 2010b; Yang and Khangaonkar 2010; Khangaonkar and Yang 2011). The term embedded is used to reflect that existing grid in SSM for the Skagit–Padilla Bay domain was replaced with approximately an order of magnitude finer resolution grid while retaining the original SSM intermediate-scale grid over the rest of the domain. The finer-scale Skagit–Padilla Bay unstructured model grid with resolution that varies from about 10 m near the river mouth to about 500 m in Saratoga Passage is shown in Figure 3.

The SSM uses the Smagorinsky scheme for horizontal mixing (Smagorinsky 1963) and the Mellor-Yamada level 2.5 turbulent closure scheme for vertical mixing (Mellor and Yamada 1982). Bottom stress is computed using a drag coefficient assuming a logarithmic boundary layer over a bot-

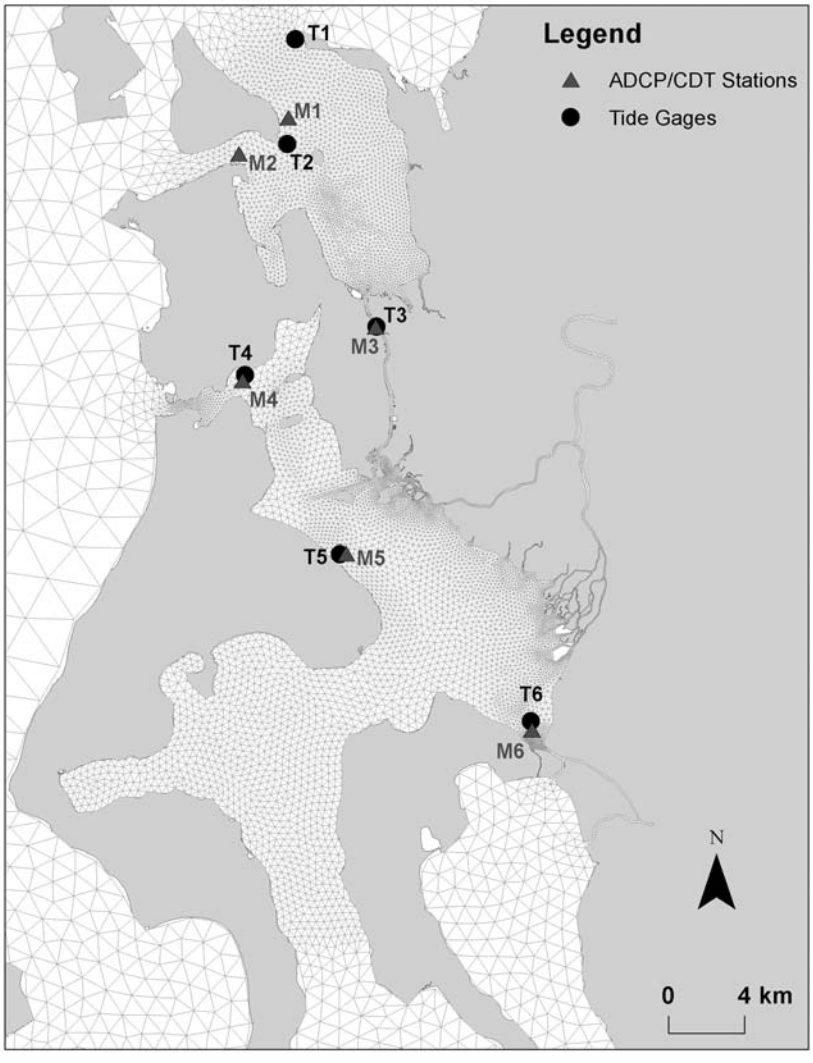

Figure 3. Fine-scale finite volume FVCOM model grid of the Skagit-Padilla Bay within the intermediate-scale SSM grid along with water-quality monitoring stations

tom roughness height Z_0 of 0.001 m. The upgraded model grid size is nearly double that of the original SSM and consists of 17,360 nodes and 28,655 elements. A mode-splitting numerical approach is used to solve the governing equations in depth-averaged two-dimensional barotropic external mode and 3-D baroclinic internal mode. A time step of 0.5 seconds was used for the external barotropic mode and 2.5 seconds for the internal mode. A sigma-stretched coordinate system is used in the vertical plane with 10 terrain-following sigma layers distributed using a power law function with an exponent P_Sigma = 1.5. This provides more layer density near the surface with nearly 50% of the layers occupying the upper 35% of the water column. This scale and the selected time step(s) allows sufficient resolution of the various major river channels and tidal marsh bathymetry while allowing year-long simulations within 48 hours of run time on a 120-processor cluster computer. The bathymetry was derived from a combined data set consisting of data from the Puget Sound digital elevation model and high-resolution light detection and ranging bathymetric data collected by Skagit River System Cooperative and U.S. Geological Survey (USGS) in the Skagit Bay tidal flats. The light detection and ranging data have a horizontal resolution of 1.8 m by 1.8 m and a vertical resolution of 0.15 m. The bathymetry was smoothed to minimize hydrostatic inconsistency associated with the use of the sigma coordinate system with steep bathymetric gradients. The associated slope-limiting ratio $\delta H/H = 0.1$ to 0.2 was specified within each grid element following guidance provided by Mellor et al. (1994) and using site-specific experience from Foreman et al. (2009), where H is the local depth at a node and δH is change in depth to the nearest neighbor. The smoothing procedure also includes adjustment of bathymetry applied to depths below 50 m in Puget Sound and near the Skagit and Padilla Bay tide flats to ensure that the individual basin and the total domain volumes remained with 1% of the original values.

One of the challenges of the SSM has been the second open ocean boundary located at the northwest corner of the model domain in Georgia Strait. This open boundary results in a net inflow to the model through the narrow section at the northwest corner representative of the connection to Johnson Strait. The magnitude and vertical distribution of this inflow has not yet been characterized through data collection and analysis. Also, the boundary salinity and temperature data in the SSM were previously specified using only limited data from within Georgia Basin and may not have accurately represented Johnstone Strait boundary properties. A series of tests were conducted with varying boundary channel configurations resulting in differing magnitudes of exchange but the influence on the inflow and circulation to the Puget Sound portion of the domain was relatively small. Given that the volume flux across this boundary is still under investigation, and to eliminate the possibility of introducing error associated with estimated inaccurate boundary conditions, in this application we simplified the setup by closing off the northern boundary at the entrance to Johnstone Strait after confirming that the exchange flow and hydrodynamic calibration for the Puget Sound region were still relatively unaffected. This affects the model's ability to predict potential changes in exchange flow through the Georgia Strait boundary and Johnstone Strait. We have assumed that sea level rise (SLR) induced changes in estuarine exchange with the Pacific Ocean will be dominated by flow through Strait of Jun De Fuca and that predictions in the Skagit Basin will not be affected by the above simplification.

Model Validation—Year 2008

As a preparatory model validation step, the existing SSM was applied for the year 2008, and the results were compared with monthly monitoring data collected by Ecology over the larger Puget Sound scale. The error statistics of water surface elevation, salinity, and temperature were computed at the stations indicated in Figure 2, and were found to be comparable to calibration results from 2006 with relative water surface elevation errors of less than 10% at all stations and salinity errors varying between 1 and 3 psu. The SSM was then upgraded as described previously whereby the existing intermediate-scale grid of Skagit-Padilla Bay region was replaced with a fine grid that required a corresponding reduction

in time step by a factor of 4 (i.e., to comply with the Courant-Friedrichs-Levy stability criterion). In addition, because temperature simulation in the intertidal zone with wetting and drying has not yet been incorporated, and given the focus of this investigation on salinity and transport, heat flux and temperature simulation were turned off as a simplification. The upgraded SSM was applied for the year 2008, and error statistics for water surface elevation, velocity, and salinity were regenerated to ensure that the overall quality of model performance was retained over the Puget Sound domain (see Table 1). The error ranges are of the same order of magnitude as those presented in Khangaonkar et al. (2012) using 2006 data at the Puget Sound stations. An average bias of approximately -1 psu was noted in simulated salinity results with predicted salinities lower than observed data. An example of comparison of simulated water surface elevation, salinity, and temperature with measured data at one of the Puget Sound calibration stations (Green Bank location in Saratoga Passage—SAR003) located near the southern end of the Skagit-Padilla Bay study area of interest is presented (Figure 4).

Operated as a standalone model forced using measured data at the boundaries, the Skagit Bay portion of the model has been calibrated previously using data from years 2005 and 2006 corresponding to low and high-river-flow periods respectively (Yang and Khangaonkar 2009, Yang and Khangaonkar 2007). In the model setup presently embedded within the SSM framework, the tidal circulation for the Skagit and Padilla Bay region is now governed by the water surface elevation and phase computed internally as part of the SSM. Because of the existence of large tidal mudflats in the near-shore regions, wetting and drying of

TABLE 1. Hydrodynamic model validation error statistics at selected locations in Puget Sound 2008.

(a) Model calibration error statistics for water surface elevation.

Station	ME (m)	MAE (m)	RMSE (m)	RME (%)
Port Angeles	-0.13	0.25	0.30	7.76
Friday Harbor	-0.27	0.27	0.32	8.47
Cherry Point	-0.22	0.26	0.30	6.82
Port Townsend	-0.22	0.26	0.30	7.16
Seattle	-0.22	0.28	0.33	6.37
Tacoma	-0.20	0.25	0.30	5.57
Mean	-0.21	0.26	0.31	7.03

MAE = mean absolute error; RMSE = root mean square error.
RME = mean error relative to tidal range at each site.

(b) Model validation error statistics for salinity at the designated sub-basin stations in Puget Sound.

Region	Location	ID	RMSE (psu)	Bias (psu)	SD (psu)
South	Budd Inlet	BUD001	1.95	-1.37	1.15
South	Gordon Point	GOR001	1.40	- 1.29	0.53
Central	Commencement Bay	CMB003	1.72	-0.97	1.40
Central	Sinclair Inlet	SIN001	2.33	-1.98	1.23
Central	West Point	PSB003	0.92	-0.38	0.67
Hood Canal	Hood Canal North	HCB010	0.87	-0.80	0.33
Whidbey Basin	Saratoga Passage	SAR003	1.15	-0.93	0.67
SJdF	Admiralty Inlet Entrance	ADM002	0.87	-0.81	0.31
Bellingham Bay	Bellingham Bay	BLL009	2.02	-0.16	1.47
		Mean	1.47	-0.96	0.86

RMSE = root mean square error; Bias = mean of paired differences (modeled–observed).
SD = standard deviation of paired differences (modeled–observed).

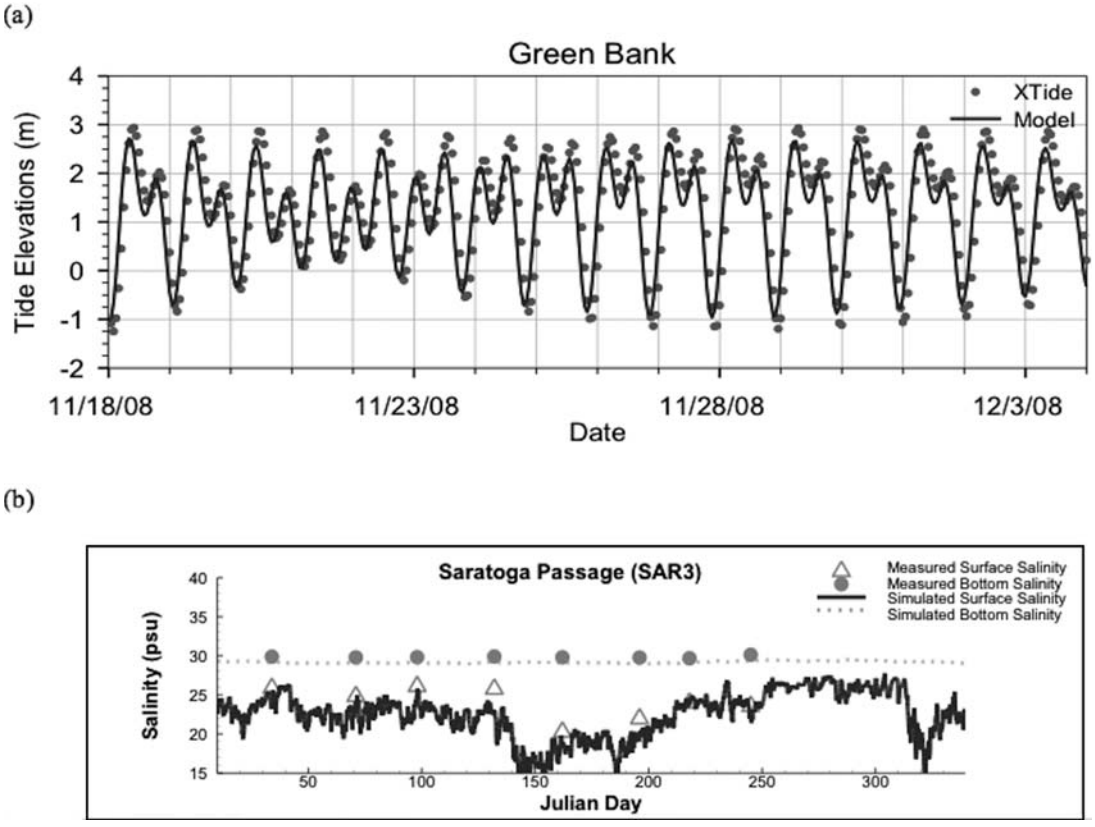

Figure 4. Example of SSM model validation. Comparison of simulated tides and salinity with XTide, and monthly monitoring data collected by Ecology at the Puget Sound Saratoga Passage station SAR003.

the intertidal zone were included in the model. A water depth of 20 cm was used as the dry-cell criterion in the model (i.e., when the depth fell below 20 cm, the model assumed that element was dry). Model performance in the near-shore locations within Skagit and Padilla Bay regions was tested using data collected simultaneously for the adjacent basins. The short 2-week duration effort in 2008 included tidal elevations (pressure gage), currents (Acoustic Doppler Current Profiler), and salinity profiles collected during deployment and recovery at the stations shown in Figure 3. Model validation was conducted by comparing predicted water surface elevation, salinity, and velocity time histories to measured data at stations covering the full neap-spring range of tidal characteristics for the period November 18, 2008 to December 4, 2008. The pressure gage and current measurements at the intertidal location T6 failed, and similarly current measurements in the Swinomish Channel M3 did not pass quality assurance/quality control likely impacted by the narrow channels, proximity to the banks, and periodic wetting and drying.

A comparison of measured and simulated tides and currents at one of the stations (station 5) located in Skagit Bay near the mouth of the North Fork of Skagit River is presented (Figure 5). The results were of a similar level of quality at stations T1/M1, T2/M2, and T4/M5 respectively. A comparison of measured and simulated salinity profiles at various stations in both the Skagit and Padilla Bay regions that were collected during the deployment and recovery of instruments is also shown (Figure 6). The figure shows salinity variation from the values of around 30 psu in the near bottom waters of Padilla Bay bordering Georgia Strait to increasing influence of freshwater in the near-shore stations in Skagit Bay. Model error

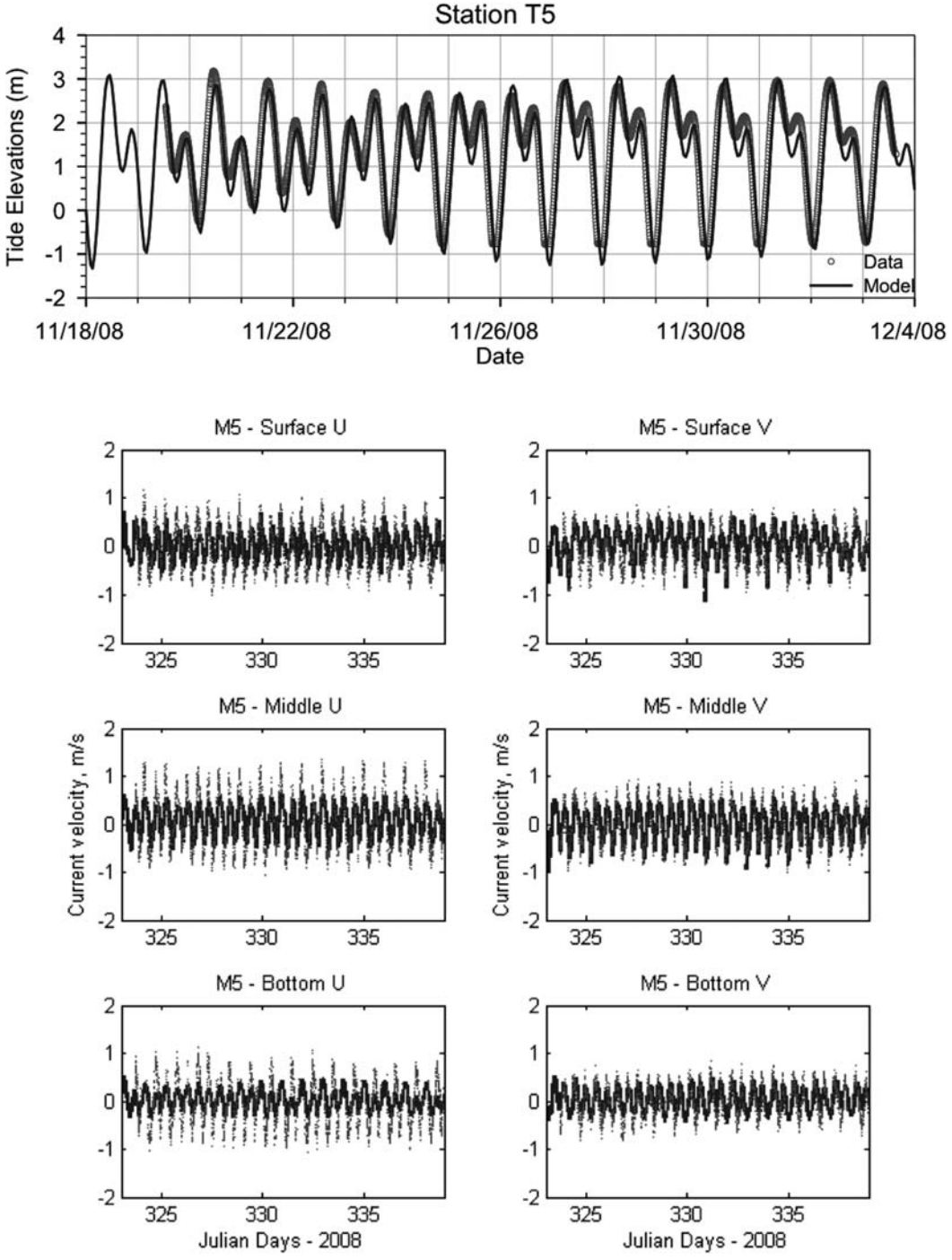

Figure 5. Comparison of simulated tides (T5) and currents (M5) at a representative station in Skagit Bay. T5/M5 station is located in the channel along Whidbey Island immediately west of the Skagit Bay tide flat at a depth of 34 m.

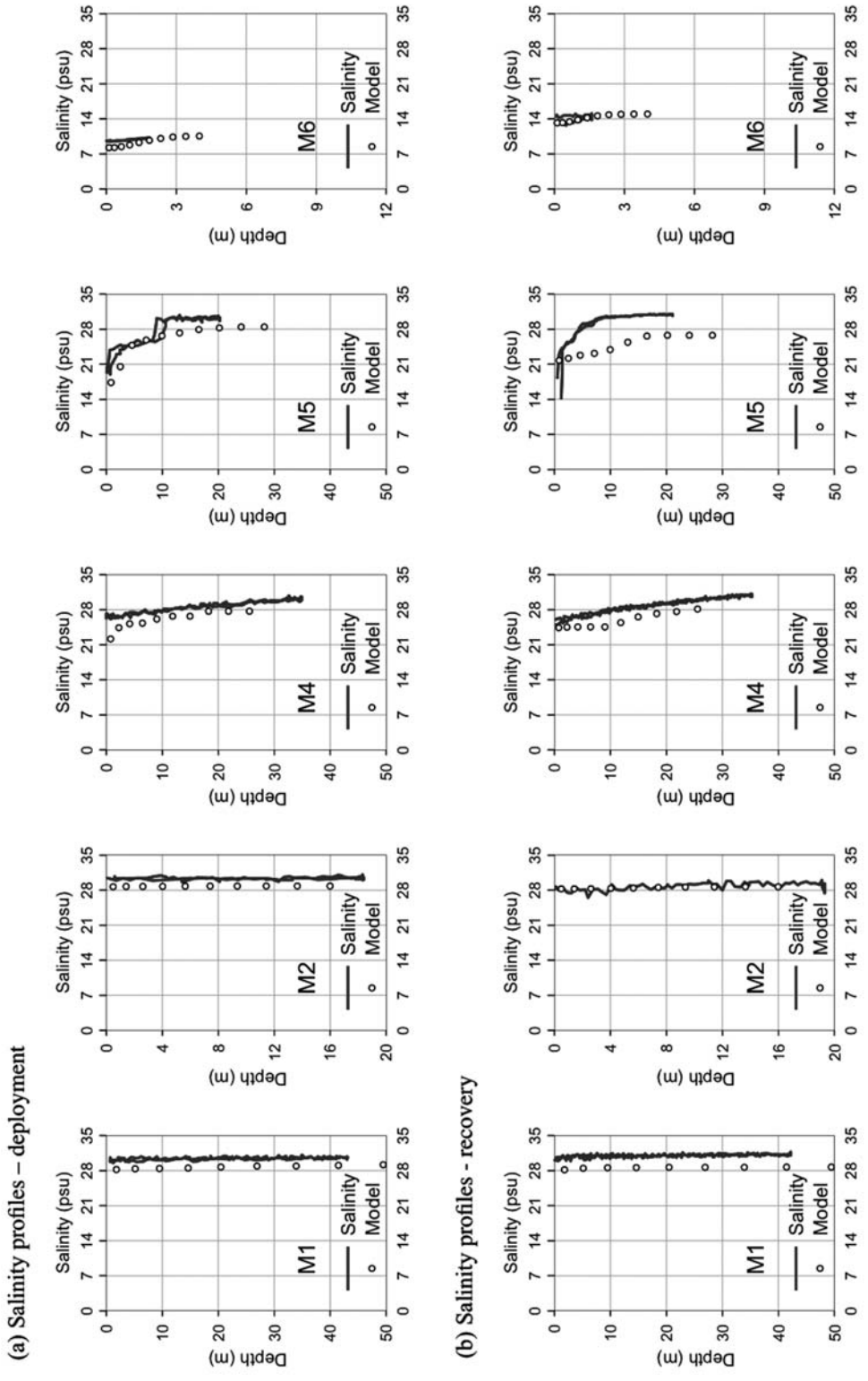

Figure 6. Comparison of simulated salinity and measured data collected during deployment and recovery of instruments in Skagit and Padilla Bay regions of Puget Sound and Georgia Basin in November 2008.

TABLE 2. Hydrodynamic model validation error statistics at tide and currents at Skagit-Padilla Bay monitoring stations (November 2008).

(a) Model calibration error statistics for water surface elevation.

Station	ME (m)	MAE (m)	RMSE (m)	RME (%)
T1	-0.44	0.44	0.48	13.65
T2	-0.28	0.30	0.34	9.89
T3	-0.14	0.18	0.21	6.14
T4	-0.13	0.23	0.27	6.69
T5	-0.17	0.26	0.30	7.69
Mean	-0.23	0.28	0.32	8.81

MAE = mean absolute error; RMSE = root mean square error.
RME = mean error relative to tidal range (magnitude of change in tidal elevation) at each site.

(b) Model calibration error statistics for velocity components U and V respectively.

	U - RMSE (m/s)			U - RME (%)		
Station	Surface	Middle	Bottom	Surface	Middle	Bottom
M1	0.24	0.0	0.20	19.91	16.93	15.41
M2	0.36	0.36	0.44	12.80	16.30	14.67
M4	0.31	0.17	0.29	17.53	10.19	16.36
M5	0.38	0.35	0.34	16.40	13.40	14.06
Mean	0.30			15.33		

	V - RMSE (m/s)			V - RME (%)		
Station	Surface	Middle	Bottom	Surface	Middle	Bottom
M1	0.19	0.20	0.21	15.00	14.83	15.85
M2	0.25	0.25	0.24	19.01	21.59	15.94
M4	0.17	0.20	0.24	18.27	13.35	16.36
M5	0.25	0.27	0.25	11.97	12.66	12.98
Mean	0.23			15.65		

U-RMSE = x component velocity root mean square error.
V-RMSE = y component velocity root mean square error.
U-RME = x component velocity error relative to magnitude of current variation.
V-RME = y component velocity error relative to magnitude of current variation.

statistics for water surface elevation and currents are presented (Table 2). Overall, the model errors for tide are within 10% of the tidal ranges from mean lower low water to mean higher high water. Average velocity errors in the x-direction (U) and y-direction (V) components are less than 0.3 m/s and average relative velocity errors are less than 15%. The signatures of neap-spring tidal cycle and diurnal inequality were observed in the collected data as well as model results. The model appears to capture the overall interaction between surface freshwater plume and bottom salt water during the tidal cycle. A bias was noted where in combination with slightly lower than observed predicted incoming salinities from Puget Sound/Georgia Basin and high mixing near the tide flats, the model results show lower near-bed salinities and higher than observed surface salinities. Sensitivity tests conducted as part of calibration showed that the currents and mixing in Skagit Bay were highly sensitive to wind, and the lack of site-specific wind data is believed to be a major source of the velocity and salinity errors. Velocity vector and salinity contour maps for surface and bottom layers showing the direction of residual currents and salinity distribution based on hourly results averaged over the year 2008 are provided in Figure 7. Salinity contours show that the bottom salinities in the basin are maintained approximately at 30 psu by transport of marine water from Puget

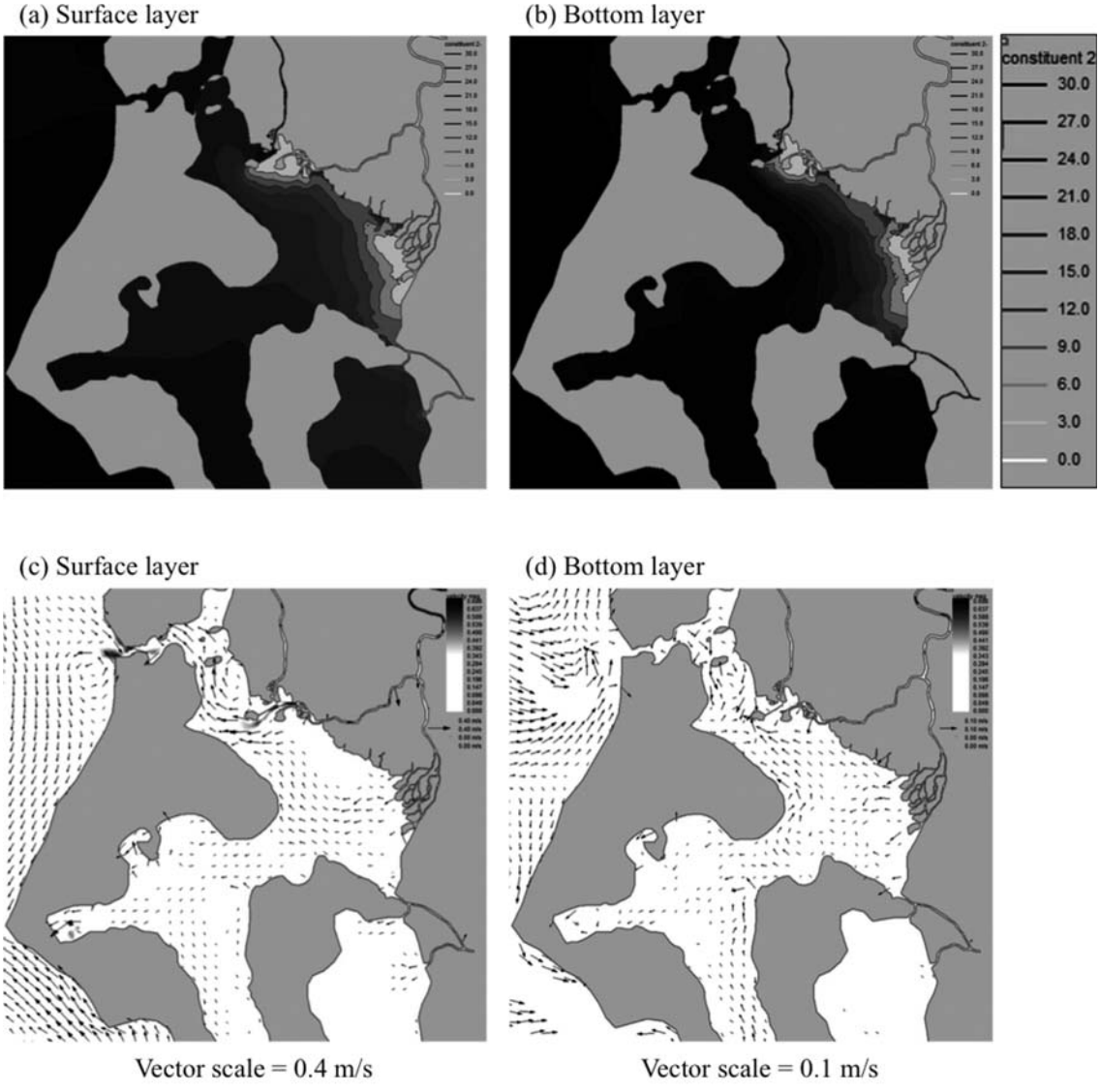

Figure 7. (a) and (b) Salinity contours in the surface and bottom layers based on average of hourly simulation results over the Year 2008. (c) and (d) Residual currents in Skagit Bay showing net transport through the system to the north also coputed as year 2008 average based on hourly results. (For plotting clarity, vectors > 0.7 m/s in the river forks and the western shores of Whidbey Island were not plotted.)

Sound via Saratoga Passage into the deep channel of Skagit Bay and then exiting through Deception Pass. Surface salinities in Skagit Bay are dominated by the freshwater plume (Figure 7a, b). The net outflow from the basin to Puget Sound via Deception Pass is noticeable in the velocity vector plots in Figure 7 (c, d).

Results

Skagit and Padilla Bay Responses to Future Sea Level and Hydrology

Future (Year 2070) Freshwater Inflows to the Salish Sea—Future climate assessments for the PNW have been conducted by the University of

Washington Climate Impacts Group, based on global climate model simulations corresponding to emissions scenarios B1, B2, A1B, B2, and A1F1 (varying from low emissions to high emissions) per the Intergovernmental Panel on Climate Change Fourth Assessment Report. Although no significant changes in annual precipitation are projected for the PNW region, substantial seasonal variations in precipitation are expected with wetter winters and springs and drier summers. Hydrologic modeling studies show that projected changes in air temperature (an increase of approximately 5.8°F for the moderate emissions scenario A1B in comparison to historical average temperature for water years 1916 to 2006), and seasonal variation in precipitation are likely to significantly alter the hydrology of most rivers discharging to the Salish Sea, including the Skagit River, resulting in more severe extreme hydrology events (e.g., floods and low flows) (Hamlet et al. 2010a).

Future hydrologic conditions for the purpose of this analysis were river and watershed stream flows representative of a selected future year, estimated based on the moderate emissions scenario A1B. Hydrologic simulations of historic and future river flows for the major rivers were conducted using the Variable Infiltration Capacity hydrologic model (Liang et al. 1994) for the years 2010 to 2069 based on emissions scenario A1B (Hamlet 2010b, Lee and Hamlet 2013). Because of uncertainty in future climate models and inter-annual variability in hydrology, using a single calendar or water years' worth of stream-flow predictions was deemed inadequate. To compensate for this variability, and provide a representative future hydrograph, we decided to average 5 years of daily stream-flow projections from 2065 to 2069 and designated it as the year 2070 estimate. Estimates of hydrologic loads from all other smaller rivers and watershed and wastewater streams entering the Salish Sea then were developed through a combination of regression and scaling techniques based on watershed areas described in Roberts et al. (2014) and Khangaonkar et al. (2012).

It is important to note that the freshwater loads to the Salish Sea for the year 2008 were based on measured records while the year 2070 flow rates are based on future hydrological simulations. Although annual average stream flows did not show a noticeable trend into the future, several rivers showed an increase in maximum annual (or peak) stream flow and a decrease in summer base flows. In general, future stream-flow predictions also showed considerable inter-annual variability, which may be one explanation for the fact that the aggregate freshwater inflow rates estimated for the 2070 simulation are different (i.e., notably higher) relative to the year 2008 records. Annual average of freshwater inflow to Salish Sea regions for years 2008 and 2070 taking into account all 19 major rivers, 45 watershed streams, and 95 wastewater streams is presented in Table 3. The aggregate river and water shed flows estimated for 2070 are 13% higher in Puget Sound and nearly 29% higher in Georgia Basin relative to 2008 flow rates. The estimated average flow rate for the Skagit River, the largest freshwater discharge to Puget Sound for 2070 is also approximately 13% higher than the 2008 flow rate. The 2070 estimate for wastewater treatment plant discharges includes the new regional Brightwater treatment plant effluent discharge, which became operational in 2011. The 2070 wastewater discharge rates are nearly double (85% higher) than the 2008 wastewater discharge rates to the Salish Sea. These increases reflect the effects of projected population growth, per capita wastewater contributions, potential changes in treatment technology, and wastewater treatment plant capacity increase projected in the region.

A comparison of Skagit River hydrographs for year 2008 and 2070 is shown as an example (Figure 8). The change in hydrograph characteristics is notable in that, during the winter and spring months from December through May, the future flows are nearly 80% higher in the Skagit Basin. The future flows do not peak in late spring/early summer months of May and June as there is no high spring flow in the future associated with snowmelt because of the projected loss of glaciers. Flows during the summer months of June, July, and August in the future are correspondingly lower. The operation of hydropower dams and associated maintenance of minimum summertime streamflows results in 7Q10 low flows of similar magnitudes in the present as well as future conditions.

TABLE 3. Annual average rates of freshwater inflow to Salish Sea for years 2008 and 2070.

Puget Sound			
Year	Skagit River[b] Flow m^3/s	Aggregate Wastewater Treatment Plant Flow Puget Sound m^3/s	Aggregate River and Watershed Flows Puget Sound m^3/s
2008	447	14	1,289
2070	504	26	1,456
Relative Increase	13%	86%	25%
Georgia Basin			
Year	Fraser River[b] Flow m^3/s	Aggregate Wastewater Treatment Treatment Plant Flow Georgia Basin m^3/s	Aggregate River and Watershed Flows Georgia Basin m^3/s
2008	2,755	18	4,374
2070	3,278	33	5,643
Relative Increase	19%	83%	29%

[a] Time histories of 19 major rivers, 45 watershed streams, and a total of 95 wastewater treatment plant flows were summed and averaged over 365 days to provide the freshwater inflow rates for years 2008 and 2070 respectively.
[b] Skagit River is the largest river to discharge to Puget Sound.
[c] Fraser River is the largest river to discharge to the Georgia Basin region in Canadian waters.

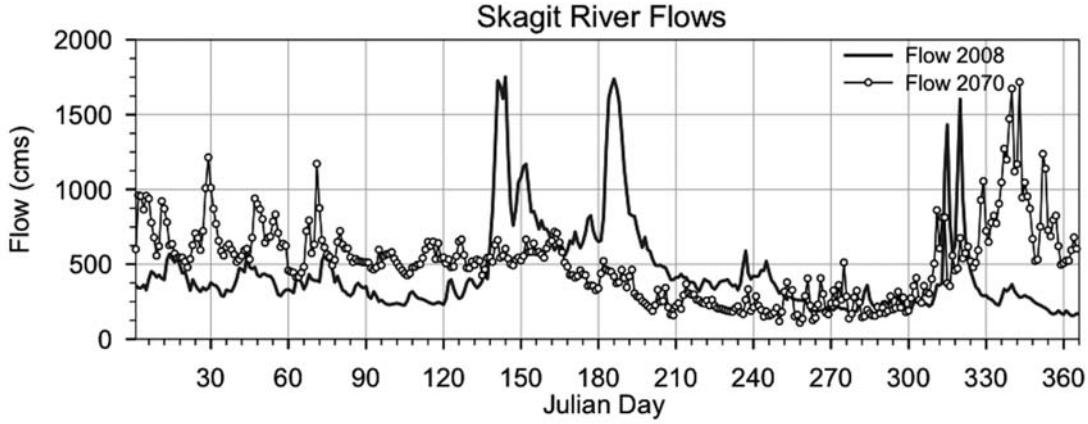

Figure 8. Skagit River Flow. Comparison of year 2008 flow time history with estimate for year 2070.

Future (Year 2070) Projected Mean Sea Level Rise—Local sea level rise projections for the coastal waters of Washington have been re-assessed based on the combined effects of global sea level rise and factors such as vertical land deformation and seasonal ocean elevation changes due to atmospheric circulation (Mote et al. 2008). The results indicate that projected global SLR of 26 to 59 cm by year 2100 included in the IPPC Fourth Assessment Report for the highest emission scenario was likely to be an underestimate for the PNW region as it did not take in to account factors such as rapid ice loss in Greenland and Antarctica. The SLR estimates for the west coast states including those in the PNW were recently revised through a National Research Council effort jointly sponsored by the states of Washington, Oregon, and California, the U.S. Army Corps of Engineers, the National Oceanic and Atmospheric Administration, and the U.S. Geological Survey (NRC 2012). Polynomial fits to the SLR projections for years 2030, 2050, and 2100 presented in

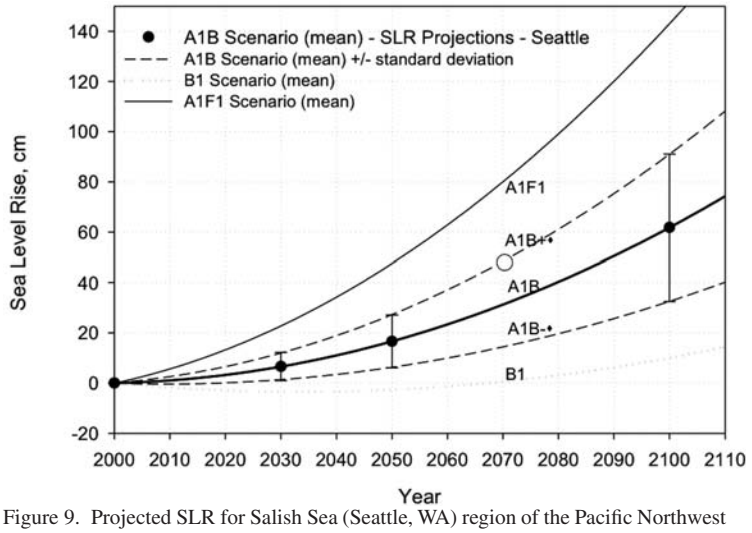

Figure 9. Projected SLR for Salish Sea (Seattle, WA) region of the Pacific Northwest for A1B, B1 and A1F1 scenarios (Source: NRC 2012). The upper and lower bounds of the modelrate emmisions scenario A1B are indicated with (- - -) dashed line.

the NRC report were reproduced (Figure 9). The projections are in the form of computed SLRs (i.e., means ± σ) for the Pacific coast from the gridded data presented in Pardaens et al. (2010) for the A1B scenario relative to year 2000. Also plotted in Figure 9 is the range of mean SLR predictions varying from the low emissions B1 scenario to the high emissions scenario A1F1. For the year 2070, estimates vary from mean SLR of zero (the low emissions scenario B1) to 80 cm (the high emissions scenario A1F1). For this analysis based on the moderate emissions scenario, we have selected to use the upper bound of the A1B SLR estimate of 48 cm.

Change in Salinity Distribution and Circulation as a Result of 2070 SLR and Flows—The Skagit-Padilla Bay system is influenced by the stratification and tidal elevations at the basin entrances at Deception Pass, Saratoga Passage, and Padilla Bay in Puget Sound and Padilla Bay. These regions are also affected by the SLR and changes in freshwater inflows. The SSM with embedded Skagit-Padilla domain was used assess the magnitude of the projected change in circulation and salinity in this system relative to year 2008 conditions. The SSM was applied using estimated future hydrologic loads from all major rivers, watershed, and wastewater streams corresponding to year 2070. The open boundary water surface elevations at Strait of Juan de Fuca were raised by 0.46 m relative to year 2008 to reflect the SLR (48 cm relative to year 2000). All other model parameters including wind and open boundary salinity and temperature profiles were left at the 2008 values.

The results show that the effect of SLR on Puget Sound in addition to the increase in mean sea level of 0.46 m also results in amplification of tidal peaks varying from the incident SLR of 0.46 m near the entrance to the Strait of Juan de Fuca to as high as 0.67 m at selected inner locations with sharp changes in channel direction resulting in higher pressure gradients. These results do not include inundation of shallow coastal areas beyond the model shoreline as a simplification under the assumption that most of the larger estuarine flood plains in the Salish Sea are protected by perimeter dikes. The projected increase in mean water depth and the change in salinity gradient have the potential to affect the residual circulation and exchange with the Pacific Ocean based on theoretical formulations for partially mixed and fjordal estuaries (McCready et al. 2004, Khangaonkar et al. 2011). Tidally averaged inflows to the basin were computed over transects across the Strait of Juan de Fuca, Admiralty Inlet, Hood Canal, and Possession Sound (entrance to Whidbey Basin) using 2008 and 2070 simulations and are listed in Table 4. The results predict ≈ 4% increase in the inflow of upwelled marine water into the Salish Sea domain through the Strait of Juan de Fuca, a 2% increase in inflow of saline waters to Puget Sound over Admiralty Inlet, and ≈ 3% increase of inflow of saline water from Puget Sound to Whidbey Basin for the year 2070 future scenario examined.

Examination of simulated salinity time histories at Ecology monitoring stations shown in Figure

TABLE 4. Mean annual inflows to Salish Sea estimated from the analysis of the year 2008 and 2070 model simulations.

Sub-basin and reach	Mean annual tidal inflow[a] year 2070 (m^3/s)	Mean annual tidal inflow[a] year 2008 (m^3/s)	Relative increase in mean tidal inflow to the sub-basins[b] (m^3/s)
Strait of Juan de Fuca	140,500	135,189	3.93%
Admiralty Inlet to Puget Sound	18,565	18,180	2.12%
Whidbey Basin (inflow through Possession Sound)	4,295	4,211	1.99%
Hood Canal	6,450	6,254	3.13%

[a] Inflow corresponds to the tidally averaged volume flux of saline water which enters the basin through the deeper layers of the water column below the depth of zero motion. Outflow consists of upwelled water mixed with freshwater discharges and occurs through the upper layers.

[b] Relative increase in mean tidal inflow is based on future conditions scenario of 0.46 m of SLR and estimated hydrological loads corresponding to A1B emissions scenario.

2, which are sufficiently away from the effects of river plumes, shows that the mean salinities averaged over year-long duration are relatively unchanged (<< 1 psu change at all stations). Although freshwater inflow estimated for the year 2070 tests is significantly higher, it is still small relative to residual tidal exchange flow that enters Puget Sound over Admiralty Inlet. The ratio of aggregate freshwater discharge to Puget Sound to mean tidal inflow over Admiralty Inlet, which was ≈ 1:14 for 2008, is a slightly lower at ≈ 1:13 for year 2070 conditions because of higher freshwater inflow. The dilution and mixing of the increased freshwater inflow with the tidal exchange flow results in only a small reduction in salinity of 0.3 psu in the surface layer, averaged over the entire domain. The effects of SLR and increased river flow appear to counteract one another when year-long averages of salinity are compared. The effect of SLR alone on salinity was to increase the saline water inflow to Puget Sound while the higher amount freshwater at the surface reduced the surface water salinity. The effect of the presence of larger amount of freshwater in the surface layer also affects bottom salinities because of reflux and mixing at the sills within Puget Sound. Consequently, the effects of changes to freshwater and estuarine exchange flows are felt more directly at the near-shore intertidal sites where the water column is well mixed. Figure 10 shows frequency plots of salinity at three representative near-shore sites (N1, N2, and N3; Figure 3) selected from within the estuarine emergent marsh zones of importance to near-shore habitat restoration actions in Padilla Bay and Skagit Bay respectively. At station N1 close to the mouth of North Fork, the results show that in year 2008, salinity was predicted to be less than 0.5 psu 90% of the time, while in 2070, the 90th percentile salinity was a higher at 1.8 psu. At station N2 near the mouth of South Fork, the 90th percentile salinity level in year 2008 is predicted at 4.6 psu, while a higher value of 5.7 psu is predicted in year 2070. These results confirm that during the low-flow summer months the near-shore salinities in Skagit Bay are predicted to be higher (≈ 1 psu higher for the simulated year 2070 conditions). At station N3 in Padilla Bay, the 90th percentile salinity values in year 2070 conditions also are predicted to be higher. It is important to note also that, at stations N2 and N3, the effect of future higher flows in the winter and spring months is reflected in corresponding lower values of salinity in the exceedance curves as shown in Figure 10.

Discussion

Salinity Intrusion

Although the magnitude of marine water inflow into Puget Sound was predicted to be higher, the salinity of incoming bottom water in the future was set the same as in existing condition.

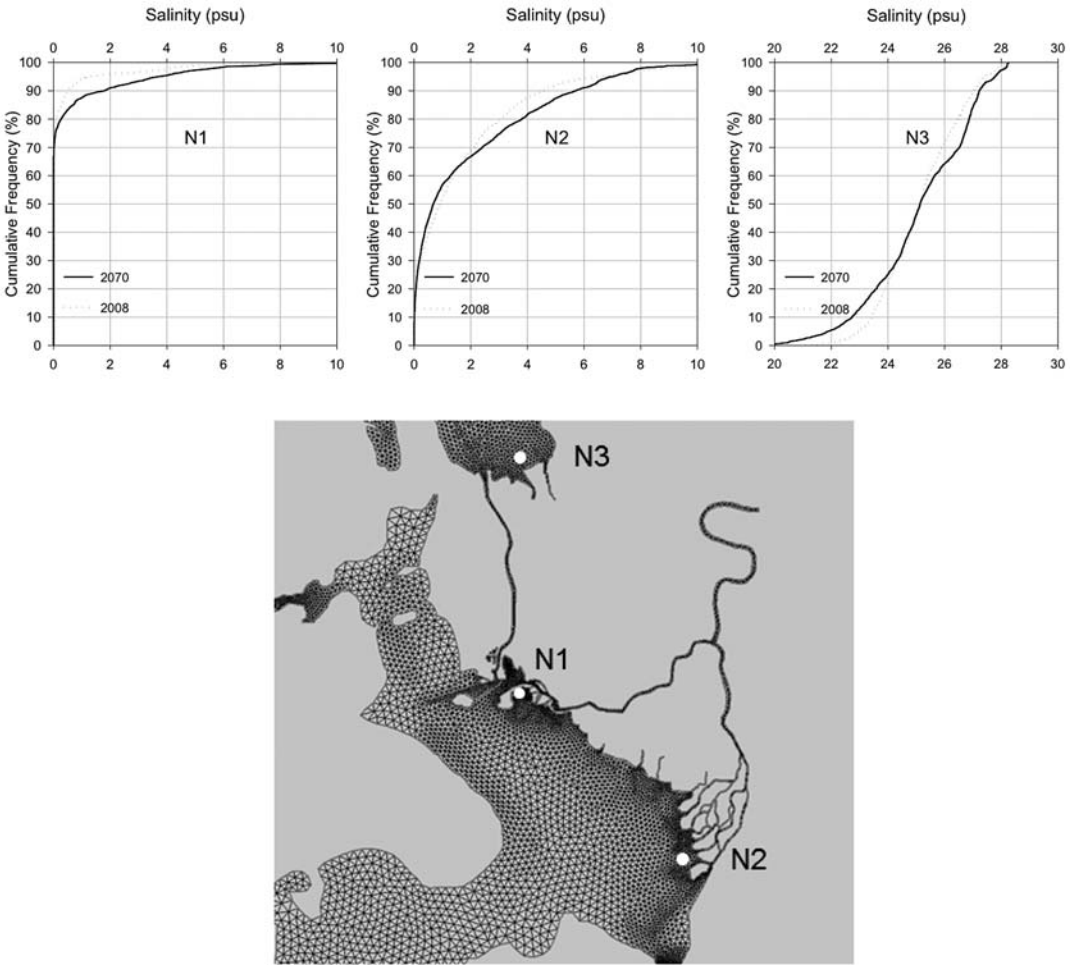

Figure 10. Cumulative frequency of salinity at near-shore stations in Skagit and Padilla Bay. N1 is near the mouth of North Fork Skagit River, N2 is near the mouth of South Fork Skagit River, and N3 is in Padilla Bay.

Consequently, the salinity boundary conditions developed for Skagit Bay and Padilla Bay for future scenarios were not a significant factor in influencing near-field salinity gradients. However, upstream salinity intrusion could still be impacted by site-specific conditions such as river slope, dikes, river-training structures, and river flow. To further examine the potential for increased salinity intrusion in the future, we examined the salinity response during the critical low-flow summer periods in the near-shore environment along a longitudinal river transect. Figure 11 shows a transect (points EDCBA) from Mt. Vernon along the South Fork of the Skagit River to Saratoga Passage. This transect was placed in the South Fork as it carries a lower fraction of the total discharge, represents the relatively less diked of the two forks of the river, and has a greater distributary deltaic structure near the river mouth. Salinity intrusion is expected to be higher along the South Forth than the North Fork branch. Predicted salinity results averaged over the low-flow month of September for years 2008 and 2070 indicate that salinity levels of 0.5 psu or higher (oligohaline conditions) generally occur downstream of point B near the mouth of the South Fork (Skagit Wildlife Area). Model predictions show a notable change in this region with average salinity levels increasing from < 0.5 psu in 2008 to a higher range from 0.5 to 2 psu for year 2070.

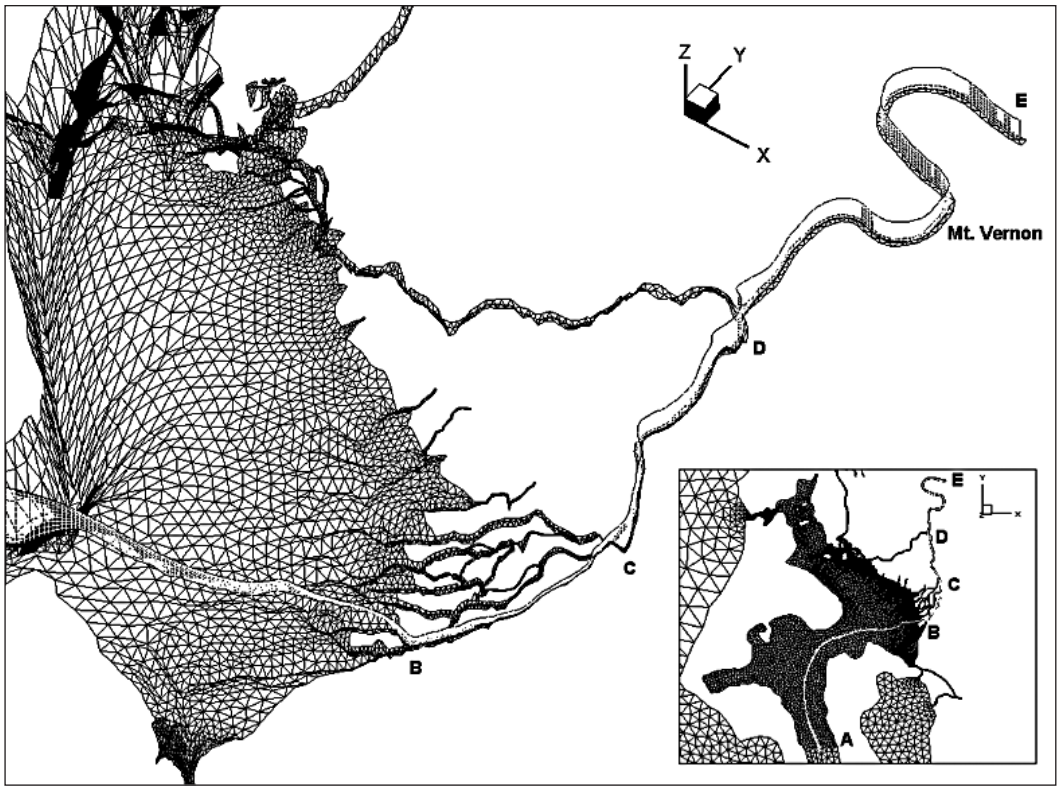

Figure 11. Near-shore model grid over the bed, and a selected transect (points EDCBA) though South Fork of Skagit River for analysis of salinity intruision.

This region of the estuary is part of the Skagit Wildlife Area intertidal marsh complex, which supports valuable salmon habitats. These habitats could undergo a change from primarily freshwater (0 to 0.25 psu) to oligohaline (0.5 to 2 psu) habitats in the future as a result of SLR. Intrusion of saline water further upstream occurs during high tide and low river flow. Salinity contour plots during the high tide in September 2008 (Julian Day 258.75) and shown in Figure 12. In 2008, the 0.5 psu salinity contour is shown to extend about 1 km upstream of point B as shown in Fig 12(a). The year 2070 simulation shows that the 0.5 psu salinity intrusion occurs approximately 3 km further upstream midway between point C near Conway and point B near the tidal marsh region. The influence of future salinity intrusion clearly does not extend beyond confluence of the North and South Forks (point D), which is about 12 km downstream of Mt. Vernon.

Transport of Skagit River Freshwater Out of the Estuary

Out-migrating salmonids are known to follow the freshwater plume transport pathways and brackish water availability at various locations in the system is an important consideration for habitat restoration planning and design (Beamer et al 2005a, 2005b). Similarly, an understanding of salt water fluxes into the estuary through the basin boundaries is also of interest given the importance of salinity gradients to the estuarine ecosystem and the possibility that the existing distribution and transport volumes may be altered as a result of future climate changes. Using the results generated, we computed volume fluxes of freshwater and saltwater based on a finite-volume mass-balance approach for the vertical transects as shown in Figure 13. For each transect, the total volume flux (total flow rate across a given transect),

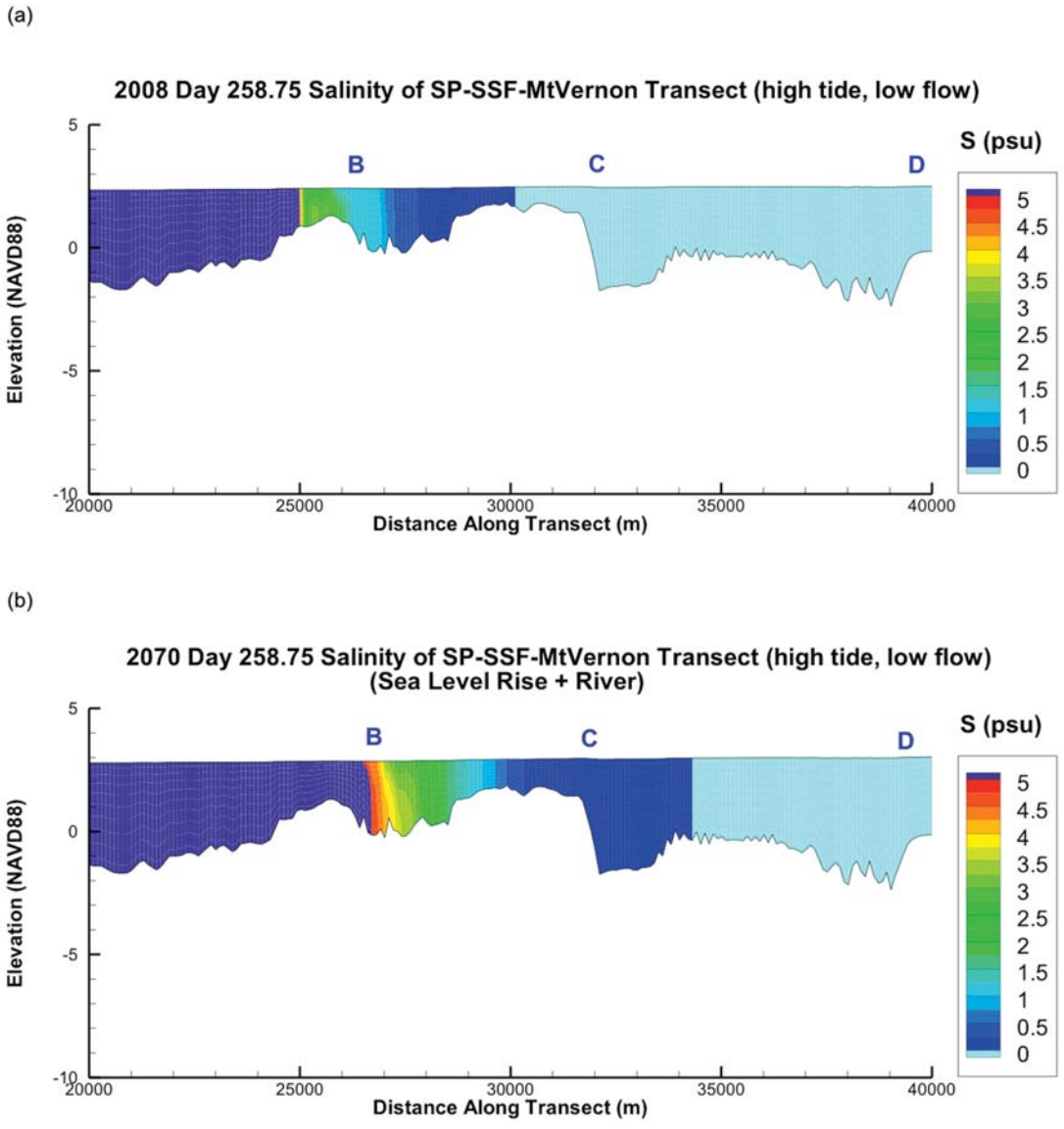

Figure 12. Simulated salinity profile along a transect (points EDCBA) for year 2008 (top panel) and 2070 (bottom panel) at low river flow time (September) and high tide. Color contours were selected such that salinity above 5 psu is in dark purple (on left) and salinity of 0 psu is in light blue (on right). The 2070 simulation included both SLR and future river discharge.

and freshwater flux (freshwater component of the total flow) were calculated.

A summary of the computed fluxes for years 2008 and 2070 respectively is provided in Table 5. The values presented are a year-long average of the flux values generated at each transect. The results show that under exiting conditions, estuarine flow is primarily exported from the basin through Deception Pass (A-A1) and Swinomish Channel (B-B1). Estuarine exchange flow enters Skagit Bay from the south and was computed at transect C-C1. A portion of Skagit River freshwater is transported out (due south) from the estuary through the surface layers at C-C1, but the net volume transport is into the estuary (due north) and is dominated by the inflow through the lay-

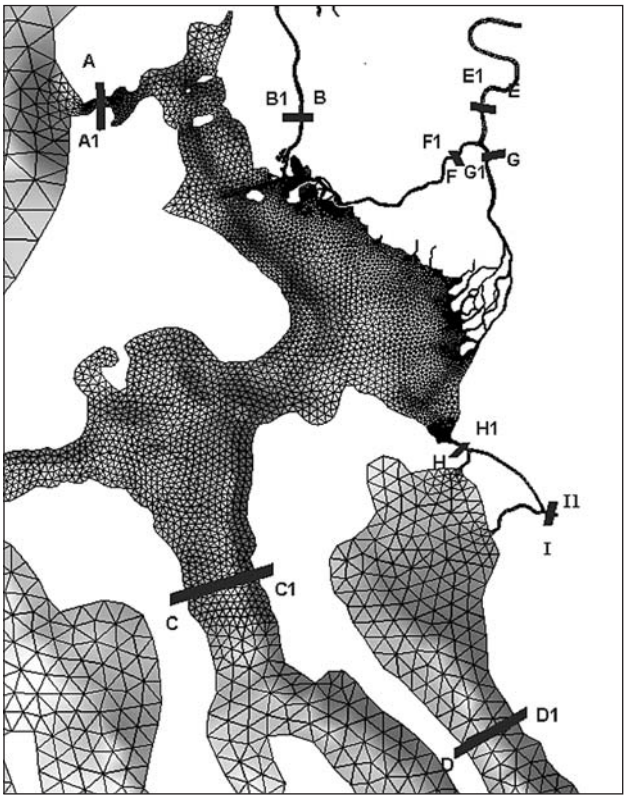

Figure 13. Locations of transects A-A1, B-B1, C-C1, D-D1, E-E1, F-F1, G-G1, H-H1, I-I1 at which the volume fluxes and salinity fluxes were calculated.

ers below the pycnocline at this location. This finding also is consistent with results published by Khangaonkar et al. (2012) where tidally averaged flow at the C-C1 location showed an outflow through the shallow brackish surface layer and inflow into the estuary through the lower layers. In this study, we used a projected year 2070 hydrograph that included a 13% increase in the total inflow (Table 1) as reflected in mean flux through EE1. Mean flux through transect C-C1, which is a combination of estuarine exchange flow and freshwater outflow, increased in 2070 (Table 5). The total flow out from the estuary appears to be predominantly through Deception Pass and is also higher in 2070 relative to 2008 because of the combined effects of increased river discharge and estuarine exchange inflow from Saratoga Passage.

During year 2008, approximately 63% of the Skagit River flow was carried by the North Fork while the South Fork carried the remaining 37%. This distribution is likely a function of flow magnitude and water depth, and the ratio changed to 60:40 for the simulated higher flows in

TABLE 5. Simulated total and freshwater flows through the selected transects in Skagit River Estuary for the years 2008 and 2070. The negative values indicate flow direction into the study domain through the respective transects while + sign indicates flow out of the domain.

	Total flow		Freshwater component of flow	
Transect	2008 Mean Flow (m^3/s)	2070 Mean flow (m^3/s)	2008 Mean flow (m^3/s)	2070 Mean flow (m^3/s)
E-E1 (T6) Skagit River Total	-445.4	-503.2	-445.4	-503.2
F-F1 (T7) North Fork	-279.06	-304.5	-279.06	-304.5
G-G1 (T8) South Fork	-166.7	-199.3	-166.7	-199.3
C-C1 (4) Saratoga Passage	-830.6	-834.0	+190.4	+183.3
A-A1 (1) Deception Pass	+1225.9	+1265.4	+303.12	+334.8
B-B1 (3) Swinomish Channel	+75.3	+78.9	+18.8	+21.8
H-H1 (9) West Pass – Stillaguamish River	+0.4	-1.7	-1.7	-6.7

year 2070. Most of the freshwater is exported from the estuary through Deception Pass to the north and Saratoga Passage to the south and only a small fraction (4%) is transported to Padilla Bay through Swinomish Channel. The simulated distributions of freshwater transport magnitudes for the year 2070 simulation are summarized in Table 6. Freshwater export from Skagit Bay to the south through Saratoga Passage decreased, and export through Deception Pass increased as a result of future conditions. The export of freshwater from Skagit Bay to Padilla Bay through the Swinomish Channel is predicted to remain relatively unchanged based on these test results.

TABLE 6. Distribution of Skagit River freshwater flow through the selected reaches of the estuary.

Flows	Transect	2008 % of Total Flow	2070 % of Total
Skagit River Inflow	E-E1	100%	100%
North Fork	F-F1	63%	61%
South Fork	G-G1	37%	40%
Freshwater Outflow			
Deception Pass	A-A1	53%	58%
Swinomish Channel	B-B1	4%	4%
Saratoga Passage	CC1	43%	36%
West Pass to Port Susan	H-H1	0%	1%

Conclusion

Amid uncertainty associated with projections of future climate and consequent impacts, sensitivity tests using numerical tools provides a convenient way to obtain quantitative information about the relative magnitudes of change that might be expected. A synoptic data-collection program with stations in the interconnected basins of Skagit Bay and Padilla Bay allowed development and calibration of an embedded high-resolution representation of Skagit-Padilla Bay system within SSM. A sensitivity level analysis was conducted using the model to assess the effects of future (2070) climate change relative to present conditions (2008) in the form of SLR (0.46 m) and altered hydrology (13% higher total flow with ≈ 80% higher winter and spring flows and lower summer flows) on estuarine circulation and transport. The results with respect to circulation and estuarine salinity are in line with the expectation that higher SLR and lower summer flows will increase salinity in the near-shore environment and result in possible upstream salinity intrusion. However the results indicate clearly that the magnitude of the changes on the Skagit River estuary is relatively small for the perturbations considered. The results show that estuarine circulation and transport subjected to the perturbations described above will result only in incremental changes to this salinity structure and inter-basin freshwater distribution and transport, and none of the simulations showed a dramatic disruption of estuarine circulation and transport in the future.

The results show that salinity levels at representative near-shore locations in the future during the low-flow summer months are predicted to be higher (≈ 1 psu higher for the simulated year 2070 conditions). This is primarily due to the predicted 3% increase in exchange flow from Puget Sound-Whidbey Basin and lower river discharge during the summer months for future conditions in year 2070. Salinity intrusion measured using contour resolution of band of 0.5 psu in the future was detected approximately 3 km further upstream relative to 2008 in the South Fork of Skagit River. Average salinity intrusion is not predicted to extend beyond Conway, Washington, below the confluence of North Fork and South Fork, and well downstream of the City of Anacortes drinking water intake near Mt. Vernon.

Sufficiently away from the effects of river plumes, the results show that the mean salinity levels averaged over a duration of one year are relatively unchanged at all stations in the greater Salish Sea study domain. Although the effect of SLR on the estuarine exchange is significant, resulting in nearly 4% increase in marine water inflow to Salish Sea, the simulated impact on near-shore salinity distribution is relatively small. This is likely because the results presented here assume that incoming upwelled Pacific Ocean marine water quality including salinity in year 2070 will be the same as that observed in year 2008. Our ability to predict future impacts to near-shore salinity gradients is therefore dependent and sensitive to the estimates of quality of Pacific Ocean marine water entering the Salish Sea system in the future.

Estuarine exchange flow or volume flux computations provided an insight into the transport pathways in and out of the Skagit River estuary. The results establish a net residual flow of marine water through the system with a magnitude ≈ 1.9 times the average river inflow, which travels north into Skagit Basin through the Saratoga Passage. This flow combined with a portion of freshwater from the Skagit River exits the basin through Deception Pass. The expectation based on examination of fish tracking data collected in the basin was that most of freshwater from Skagit River carrying the out-migrating fish exited the basin toward the north, through the Deception pass and the Swinomish Channel (Lee et al. 2010). The results in contrast show that export pathways are comparable through the north and south boundaries through the surface layers. A little over half (53%) of Skagit River freshwater is transported out to Puget Sound via Deception Pass while a comparable and significant fraction, nearly 43%, of Skagit River water is transported south to Saratoga Passage based on existing Year 2008 simulations. Only ≈ 4%, a small fraction of total freshwater delivered to the Skagit Basin makes it to Padilla Bay through the Swinomish Channel. As in the case of the salinity distribution, the transport pathways are not significantly altered for the future scenarios that we examined. These results indicate that the overall structure of oceanographic circulation and transport will likely not be significantly altered as a result of SLR and future flows especially when year-long average conditions are examined. The overall effect of SLR and hydrological modifications is to incrementally strengthen the estuarine transport through the system in the northern direction from Saratoga Passage to Deception Pass.

We do note, however, that the scenarios considered only a conservative SLR of 0.46 m and hydrology corresponding to moderate emissions scenario A1B. The simulations also included an approximation that estuarine inflow into Puget Sound and, therefore the Skagit Basin, will be at same salinity in the future. The results therefore should be treated as preliminary estimates until results from more extensive analyses become available.

Acknowledgments

This work would not have been possible without technical input and contributions from our colleagues from the Skagit Climate Science Consortium. We also acknowledge our collaborators Karol Erickson and Mindy Roberts from the Washington State Department of Ecology and Ben Cope from the U.S. Environmental Protection Agency for their encouragement and support.

Literature Cited

Babson, A. L., M. Kawase, and P. MacCready. 2006. Seasonal and interannual variability in the circulation of Puget Sound, Washington: A box model study. Atmosphere-Ocean 44:29-45.

Beamer, E., A. McBride, C. Greene, R. Henderson, G. Hood, K. Wolf, K. Larsen, C. Rice, and K. Fresh. 2005a. Delta and Nearshore Restoration for the Recovery of Wild Skagit River Chinook Salmon: Linking Estuary Restoration to Wild Chinook Salmon Populations. Appendix D of the Skagit Chinook Recovery Plan, Skagit River System Cooperative, La Conner, WA.

Beamer, E., B. Hayman, and D. Smith. 2005b. Linking Freshwater Rearing Habitat to Skagit Chinook Salmon Recovery. Appendix D of the Skagit Chinook Recovery Plan, Skagit River System Cooperative, La Conner, WA.

Beamer, E., C. Rice, R. Henderson, K. Fresh, and M. Rowse. 2007. Taxonomic Composition of Fish Assemblages, and Density and Size of Juvenile Chinook Salmon in the Greater Skagit River Estuary. Field Sampling and Data Summary Report. Department of the Army Seattle District Corps of Engineers P.O. Box 3755 Seattle, WA.

Chen C., H. Liu, and R. C. Beardsley. 2003. An unstructured, finite-volume, three-dimensional, primitive equation ocean model: application to coastal ocean and estuaries. Journal of Atmospheric and Ocean Technology 20:159-186.

Doney, S. C., M. Ruckelshaus, J. E. Duffy, J. P. Barry, F. Chan, C. A. English, H. M. Galindo, J. M. Grebmeier, A. B. Hollowed, N. Knowlton, J. Polovina, N. N. Rabalais, W. J. Sydeman, and L. D. Talley. 2011. Climate change impacts on marine ecosystems. Annual Review of Marine Science 4:11-37.

Flater, D. 1996. A brief introduction to XTide. Linux Journal 32:51-57.

Foreman, M. G. G., P. Czajko, D. J. Stucchi, and M. Guo. 2009. A finite volume model simulation for the Broughton Archipelago, Canada. Ocean Modeling 30:29-47.

Greene, C. M., D. W. Jensen, G. R. Pess, E. A. Steel, and E. Beamer. 2005. Effects of environmental conditions during stream, estuary, and ocean residency on Chinook salmon return rates in the Skagit River, Washington. Transactions of the American Fisheries Society 1562-1581.

Grossman, E. E., A. Stevens, G. Gelfenbaum, and C. Curran. 2007. Nearshore Circulation and Water Column Properties in the Skagit River Delta, Northern Puget Sound, Washington—Juvenile Chinook Salmon Habitat Availability in the Swinomish Channel. U.S. Geological Survey Scientific Investigations Report 2007-5120.

Hamlet, A. F., S. Y. Lee, N. J. Mantua, E. P. Salathe, A. K. Snover, R. Steed, and I. Tohver. 2010a. Seattle City Light Climate Change Analysis for the City of Seattle. Seattle City Light Department, The Climate Impacts Group, Center for Science in the Earth System, Joint Institute or the Study of the Atmosphere and Ocean, University of Washington, Seattle.

Hamlet, A. F., P. Carrasco, J. Deems, M. M. Elsner, T. Kamstra, C. Lee, S-Y Lee, G. Mauger, E. P. Salathe, I. Tohver, and L. Whitely Binder. 2010b. Final Project Report for the Columbia Basin Climate Change Scenarios Project. Climate Impacts Group, Seattle, WA.

Hood, W. G. 2006. A conceptual model of depositional, rather than erosional, tidal channel development in the rapidly prograding Skagit River Delta (Washington, USA). Earth Surface Processes and Landforms 31:1824-1838.

Khangaonkar, T., Z. Yang, T. Kim, and M. Roberts. 2011. Tidally averaged circulation in Puget Sound subbasins: comparison of historical data, analytical model, and numerical model. Estuary Coast and Shelf Science 93:305-319.

Khangaonkar, T., and Z. Yang. 2011. A high resolution hydrodynamic model of Puget Sound to support nearshore restoration feasibility analysis and design. Ecological Restoration 29:173-184.

Khangaonkar, T., B. Sackmann, W. Long, T. Mohamedali, and M. Roberts. 2012. Simulation of annual biogeochemical cycles of nutrient balance, phytoplankton bloom(s), and DO in Puget Sound using an unstructured grid model. Ocean Dynamics 62:1353-1379.

Liang, X., D. P. Lettenmaier, E. F. Wood, S. J., and Burges. 1994. A simple hydrologically based model of land surface water and energy fluxes for GSMs. Journal of Geophysical Research 99:14415-14428.

Lee, C., T. Khangaonkar, Z. Yang, and E. Beamer. 2010. Development of a land use planning tool for estuarine habitat protection, restoration, and cumulative effects assessment in northern Puget Sound, WA. Report PNWD 4175, prepared for the NOAA/UNH Cooperative Institute for Coastal and Estuarine Environmental Technology (CICEET). Batelle Pacific Northwest Division, Richland, WA.

Lee, S-Y., A. F. Hamlet, and E. Grossman. 2016. Impacts of climate change on regulated streamflow, flood control, hydropower production, and sediment discharge in the Skagit River basin. Northwest Science (this issue).

Mellor, G. L., T. Ezer, and L-Y Oey. 1994. The pressure gradient conundrum of sigma coordinate ocean models. Journal of Atmospheric and Ocean Technology 11:1126-1134.

Mellor, G. L., and T. Yamada. 1982. Development of a turbulence closure model for geophysical fluid problems. Review of Geophysics 20:851-875.

Mote, P. W., A. Peterson, H. Shipman, W. S. Reeder, and L. Whitely Binder. 2008. Sea Level Rise in the Coastal Waters of Washington. Report for the Climate Impacts Group, University of Washington, Seattle.

Mohamedali, T., B. S. Sackmann, and A. Kolosseus. 2011. Puget Sound dissolved oxygen model: nutrient load summary for 1999–2008. Publication No. 11-03-057, Washington State Department of Ecology, Olympia.

National Wildlife Federation. 2007. Sea-level rise and coastal habitats in the Pacific Northwest— an analysis for Puget Sound, southwestern Washington, and northwestern Oregon. Western Natural Resource Center, Seattle, WA.

National Research Council. 2011. Climate Stabilization Targets: Emissions, Concentrations and Impacts over Decades to Millennia. The National Academies Press, Washington, DC.

National Research Council. 2012. Sea-Level Rise for the Coasts of California, Oregon, and Washington: Past, Present, and Future. The National Academies Press, Washington, DC.

Pardaens, A. K., J. M. Gregory, and J. A. Lowe. 2010. A model study of factors influencing projections of sea level over the twenty-first century. Climate Dynamics 36:2015-2033.

Rice, C. A. 2007. Evaluting the biological condition of Puget Sound. Ph.D. Dissertation. University of Washington School of Aquatic and Fishery Sciences, Seattle, WA

Roberts, M., T. Mohamedali, B. Sackmann, T. Khangaonkar, and W. Long. 2014. Dissolved oxygen model scenarios for Puget Sound and the straits: impacts of current and future nitrogen sources and climate change through 2070. Publication No. 14-03-007, Washington State Department of Ecology, Olympia.

Smagorinsky, J. 1963. General circulation experiments with the primitive equations. I. The basic experiment. Monthly Weather Review 91:99-164.

Sutherland, D. A., P. MacCready, N. S. Banas, and L. F. Smedstad. 2011. A model study of the Salish Sea estuarine circulation. Journal of Physical Oceanography 41:125-1143.

Wiggins, W. D., G. P. Ruppert, R. R. Smith, L. L. Reed, and M. L.Courts. 1997. Water resources data,

Washington, water year 1997. U.S. Geological Survey, Water Data Report WA-97-1, Tacoma, WA.
Yang, Z., and T. Khangaonkar. 2006. Hydrologic and hydrodynamic modeling of the Skagit River estuary—Rawlins Road restoration feasibility study. Report PNWD 3692, prepared for the Skagit Watershed Council. Batelle Pacific Northwest Division, Richland, WA.
Yang, Z., and T. Khangaonkar. 2007. Hydrodynamic modeling analysis for McGlinn Causeway feasibility study. Report PNWD 3813, prepared for the Skagit River System Cooperative, Batelle Pacific Northwest Division, Richland, WA.
Yang, Z., and T. Khangaonkar. 2009. Modeling tidal circulation and stratification in Skagit River estuary using an unstructured grid ocean model. Ocean Modeling 28:34-49.
Yang, Z., T. Khangaonkar, M. Calvi, and K. Nelson. 2010. Simulation of cumulative effects of nearshore restoration projects on estuarine hydrodynamics. Ecological Modelling 221:969-977.
Yang, Z., K. Sobocinski, D. Heatwole, T. Khangaonkar, R. Thom, and R. Fuller. 2010. Hydrodynamic and ecological assessment of nearshore restoration: a modeling study. Ecological Modelling 221:1043-1053.
Yang, Z., and T. Khangaonkar T. 2011. Multi-scale modeling of Puget Sound using an unstructured-grid coastal ocean model: from tide flats to estuaries and coastal waters. Ocean Dynamics 60:1621-1637.

Received 1 September 2014
Accepted for publication 26 August 2015